Retrieval of an Elevation Map using UAV Imagery and Ground Control Points collected with a Low-Cost Positioning Device

R.C.T. Smits

15-06-2020

Retrieval of an Elevation Map using UAV Imagery and Ground Control Points collected with a Low-Cost Positioning Device

By

R.C.T. Smits

In partial fulfilment of the requirements for the degree of

Bachelor of Civil Engineering

At the Delft University of Technology

Supervised by:

Dr. ir. J.A.E. ten Veldhuis, TU Delft
Prof. dr. ir. N.C. van de Giesen, TU Delft

Coordinated by:

Dr. ir. R. J. van der Ent, TU Delft

Student number: 4445481
Project duration: 20/04/2020 – 17/06/2020

Preface

This thesis is written to fulfil the requirements for the degree of Bachelor of Science in Civil Engineering at the Delft University of Technology. The research is conducted to gain knowledge for the TWIGA project in sub-Saharan Africa, which is described further in this report. Originally, the research including its measurements would have taken place in the city of Kumasi, Ghana. Due to the COVID-19 circumstances, the project and measurements are done in the Netherlands in an as much as possible comparable and representative environment. Due to the fact that the goal of this report is to provide information for the international TWIGA project and because of the received help from international researchers, this report is written in English.

I would like to thank dr. ir. Marie-Claire ten Veldhuis and prof. dr. ir. Nick van de Giesen for giving us the opportunity to take part in such a project and to perform field measurements with professional equipment. Furthermore, I want to thank them for their supervision during this project. In addition, I would like to thank Jan van Til from HiView for carrying out the UAV flight and his help and responsibility. Also, a massive thanks to Jan for the processing of the elevation data and the generation of the elevation models. Next, I want to thank Andreas Krietemeyer, PhD researcher at the TU Delft, for teaching us the work methods of the low-cost receiver and the tips regarding our plan of measurements. Last, a special thanks to dr. ir. Hans van der Marel from the TU Delft for introducing us to the professional Trimble R8 receiver and the processing of the data measured with this device, and to Peter Verweij, graduate student Industrial Design Engineering at TU Delft, for helping with the set-up and the handling of the low-cost GNSS device.

Ruben Smits
Delft, June 2020

Abstract

Many countries in sub-Saharan Africa experience lack of knowledge regarding the way they deal with weather, water and climate data, which is known as geo-information. A digital elevation model (DEM), a representation of topographic surface elevations of an area, can provide necessary information for water management purposes, such as predictions of water flow directions and accumulation. Photogrammetric generation of accurate DEMs using aerial imagery methods is said to be highly dependent on reference points in the study terrain. These reference points are called ground control points (GCPs) and its information is used to correct the distortion of aerial images. Measurements of the coordinates of GCPs are performed with Global Navigation Satellite Systems (GNSS). Professional GNSS devices come at high prices, for which in most countries no budget is available. Moreover, the acquisition of GCPs is difficult in most study environments due to the high measurement requirements. In 2018, a project named TWIGA[1] started in sub-Saharan Africa, with the objective of making satellite-based geo-information available for all concerned parties. One of its research fields is a study to the use of low-cost positioning devices for hydrological purposes.

This report aimed to provide information for the TWIGA project regarding the retrieval of DEMs based on GCPs measured by a low-cost positioning device. The research question "What accuracy of an elevation model can be achieved if it is retrieved using ground control points collected by a low-cost positioning device?" was formulated. The effects of differing numbers of GCPs on the accuracy of a DEM were investigated. An area of 27 hectares including terrain elevations was studied. A UBlox positioning device, which is originally produced for mass market products such as navigation systems, was used as the low-cost option. The Trimble R8 receiver was used as the professional one, to which the results were referenced. For the caption of the aerial images an unmanned aerial vehicle (UAV) was used, the eBee Classic by SenseFly. HiView, a company with expertise in UAV flights, assisted with the measurements, aerial imagery and the generation of the different DEMs.

Analyses of the generated DEMs with varying numbers of GCPs indicated that the use of a small number of GCPs results in elevation maps with mean errors of three centimetres, being highly comparable with a DEM derived using a large number of GCPs. However, if no GCPs and thus only the internal UAV sensors are used, the retrieved model is too erroneous to be useful. In studies where the acquisition of GCPs is inconvenient and difficult, it was found to be highly recommended to use at least a small number of GCPs in order to retrieve usable elevation maps. In flood risk predictions, on the other hand, the implementation of a low-cost derived DEM needs to be researched more thoroughly, as simulations in this field require high accuracy elevation data and face high risks of disastrous events when errors occur.

[1] Transforming Water, Weather, and Climate Information through in situ observations for Geo-Services in Africa

Table of contents

List of tables

List of figures

Abbreviations

AHN	Actueel Hoogtebestand Nederland
DEM	Digital Elevation Model
DSM	Digital Surface Model
DTM	Digital Terrain Model
EGM96	Earth Gravitational Model 1996
ETRS89	European Terrestrial Reference System 1989
ETRF2000	European Terrestrial Reference Frame 2000
GCP	Ground Control Point
GIS	Geographic Information System
GNSS	Global Navigation Satellite System
GRS80	Geodetic Reference System 1980
MVS	Multi-view stereo
NAP	Normaal Amsterdams Peil
QGIS	Quantum Geographic Information System
RGB	Red, Green, Blue
RTK	Real Time Kinematic
SIFT	Scale-Invariant Feature Transform
SfM	Structure-from-Motion
UAV	Unmanned Aerial Vehicle
WGS84	World Geodetic System 1984

1. Introduction

Many countries experience lack of knowledge and information regarding the way they deal with weather, water and climate data, which is known as geo-information. Satellites and other forms of aerial imagery can provide informative maps for water and land management purposes. In a lot of these countries, affordable and innovative GNSS (Global Navigation Satellite System) techniques are desired, due to the fact that existing professional systems simply are too expensive to do measurements with (Krietemeyer, Ten Veldhuis, & Van de Giesen, 2017). This research project investigates the possibility of implementation of low-cost positioning devices in hydrological projects. The main focus will lie on projects in countries where satellite-based geo-information, which provide information services such as weather predictions, is poor and thus needed.

1.1 Problem analysis

1.1.1 Users

In Africa, the absence of accurate information services has led to a considerable vulnerability to consequences of climate change. According to TWIGA (n.d.), "few places on Earth are served worse with geo-information than Africa", while, on the other hand, Africa faces large opportunities in improving its land and water use due to its rich and fertile soils. As stated by Dr. Akinwumi A. Adesina (2019, p. 1), President of the African Development Bank, "Africa has 65% of the world's remaining uncultivated arable land, an abundance of fresh water and about 300 days of sunshine each year". Users of geo-information are highly dependent on services such as weather predictions and (local) heavy rainfall prospects. For instance, agricultural producers benefit a lot from knowing how to schedule irrigation in order to improve their crop yield and drinking water companies would be able to improve their efficiency and energy use if weather predictions were more accurate. In addition, policymakers and building companies rely on detailed geo-information in order to adapt their plans to changing weather conditions. These are only few of the many users that have an enormous potency in improving their results by having access to accurate weather and water data.

Moreover, even more crucial is the increasing risk of flood disasters in densely populated areas due to climate change effects. The city of Kumasi, the fastest growing city in Ghana, is an example. As studied by Amoateng, Finlayson, Howard, and Wilson (2018), Kumasi experiences disastrous floods at least four times a year after rainfall events, particularly as a result of "uncontrolled occupation of inland water areas by urban physical developments" (p. 1). Kumasi is located in the region of sub-Saharan Africa, one of the regions that encounters a lot of issues due to insufficient geo-information (TWIGA, n.d.). In 2018, the TWIGA project started, with the objective of providing sufficient geo-information for all concerned parties in this region by developing new methods of acquiring and processing satellite-based data (Van de Giesen, Krietemeyer, Ten Veldhuis, & Annor, 2018). TWIGA is an acronym for Transforming Water, Weather, and Climate Information through in situ observations for Geo-Services in Africa and is the Swahili word for giraffe, "an animal that derives a competitive advantage from carefully observing its environment" (Van de Giesen et al., 2018, p. 1). The TWIGA project is funded by the Horizon 2020 Research and Innovation Programme. The general aim of the Horizon 2020 programme, an initiative of the European Commission, is to bring science and innovation closer to the people who need it most (Horizon 2020, n.d.).

1.1.2 Services

One of the services the users, and citizens, would benefit a lot from, is an accurate prediction of developments of certain water flows in terms of their accumulation or direction (TWIGA, n.d.). Also,

variations in watersheds can be highly informative. This information can mostly be derived from knowledge of elevations in particular areas, which are described in digital elevation models (DEMs). According to GIS Geography (2020), a DEM is a "bare-earth raster grid referenced to a vertical datum", which is a surface of zero elevation to which heights can be referred to. DEMs are in most cases a good representation of topographic surface elevations above a certain reference level and can help provide necessary information about water and land management. For example, the slope steepness of a watershed, the direction of water flows and flood simulation (Zhang et al., 2018). However, the spatial prediction of river flood risk requires very high accuracy DEM data. Digital terrain models (DTMs) and digital surface models (DSMs) are also known as specific versions of elevation models. DTMs are in most countries synonymous with DEMs, which are surface models of which vegetation and structures are filtered out. Therefore, they are called bare-earth models. DSMs, on the other hand, are elevation models of which the tops of those buildings and trees are included. The difference between DTMs (or DEMs) and DSMs is shown in Figure 1.1. In this report, DEM is used as the generic term for such elevation models.

Figure 1.1: difference between DTM/DEM and DSM (GIS Resources, 2016).

A DEM can be retrieved from aerial images in combination with known positions of ground control points (GCPs). For instance, unmanned aerial vehicle (UAV) imagery – also known as drone imagery – can serve as input to construct a DEM, using GCPs to correct the UAV images. The methodology behind this, which is called photogrammetry, will be described in the next chapter. According to Remondino, Barazzetti, Nex, Scaioni, and Sarazzi (2011, p. 25), drones are "the low-cost alternative to the classical manned aerial photogrammetry" and next to that, the UAVs can fly at lower altitudes which result in the spatial resolution of the retrieved data to be of a higher level (Everaerts, Lewyckyj, & Fransaer, 2004). Drones are therefore ideally used in local applications rather than expensive laser scanning or radar methods, which are capable of covering large, wide areas. GCPs are visible points on the surface of which the exact coordinates (latitude, longitude and altitude) are known (OpenDroneMap, n.d.). The positions of those points are to be measured prior to the caption of the UAV images, so that all positions are exactly known before the drone camera takes the photographs. Professional, high priced GNSS devices can measure the desired information about the GCPs such as the exact position in both horizontal and vertical alignments. With this information, a DEM can be constructed. The more accurate the measured positions of the GCPs, the higher the accuracy of the DEM.

In the environments described in the previous paragraph, however, the use of professional positioning devices is most of the time too expensive. According to Krietemeyer, Ten Veldhuis, Van der Marel, Realini, and Van de Giesen (2018), the costs can exceed several thousands of dollars. Next to that, coordinates of GCPs are not always retrieved easily and accurately because of the high measurement requirements of GNSS receivers, such as the absence of canopy above the antennas and the absence of tall surrounding structures or buildings (Chen et al., 2018). With the use of low-cost

GNSS receivers, along with imagery by UAVs, measurements and eventually the retrieval of a DEM can be done in a significantly cheaper way. These low-cost GNSS devices will have a maximum price of a few hundred dollars as they were originally designed for the mass-market, for example to be used in a car navigation system (Krietemeyer et al., 2018). The risk of inaccurate measurements, however, can increase due to the fact that low-cost receivers are less accurate by default, and moreover, due to the combination of high measurement requirements and the studied areas in urban environments such as the previously mentioned city of Kumasi.

Overall, it can be said that by using affordable equipment, a lot more applications and challenges in this research field can be studied and taken into practice. Therefore, it would be a great opportunity for those users of geo-information and specifically, users of DEMs for water management purposes, to be able to use low-cost positioning devices. The knowledge and moreover, the use of satellite-based information in these environments will increase enormously in this case.

1.2 Aim and objective

The main motivation for conducting the research is to provide insight into the performances and results of low-cost positioning devices in order to possibly implement these devices in research projects where no budget is available for professional systems. The objective is to study if a DEM with an accuracy as high as possible can be retrieved from UAV imagery, corrected by measurements of different numbers of GCPs which are collected with a low-cost positioning device. In order to carry out the measurements properly and to retrieve an informative DEM, an appropriate study area which contains height differences is to be determined. Also, the determination and accuracy of the GCPs is of high importance in order to make the study area as realistic as possible for environments such as the urban, prone to flooding areas in sub-Saharan Africa. Therefore, the retrieval of a DEM without the use of GCPs is examined as well, in order to finally be able to determine the optimal number of necessary GCPs. The obtained data is evaluated through comparison with a retrieved DEM by using a professional, high priced GNSS device and the positions of the exact same ground control points. As a result, the accuracy of the low-cost retrieved DEM and with that, the usability of it in low budget projects and environments is monitored and described. The following research question for this report is formulated:

"What accuracy of an elevation model can be achieved if it is retrieved using ground control points collected by a low-cost positioning device?"

In order to achieve the goal described above, the following sub-questions are to be answered.

1. How can a DEM be derived from UAV imagery and be corrected with the known positions of GCPs?
2. How can the number of measured GCPs influence the accuracy of a low-cost retrieved DEM?
3. How can the distance between the measured GCPs influence the accuracy of a low-cost retrieved DEM?
4. How can the spatial distribution of the measured GCPs influence the accuracy of a low-cost retrieved DEM?

1.3 Approach

For this research to be conducted in a structured way, an approach was composed. First, a literature study was performed on the background of the research subject, on GNSS receivers and on the retrieval of a DEM from UAV images and GCPs via photogrammetry. Also, a study was done to an appropriate

location for the area where the measurements have been carried out. On the 13th and 14th of May, the field measurements and the UAV flight took place. Then, the processing of the retrieved data into DEMs with the two sets (professional and low-cost) of GCP positions was scheduled. In this phase, the effects of a dense, sparse and absent network of GCPs on the accuracy of a DEM were researched, to be able to answer the research questions. Lastly, the final results were analysed and discussed, in order to come up with a conclusion and recommendations eventually.

1.4 Structure

The report is structured as follows. The first chapter gives an introduction to the research and a problem analysis to describe the motivation of this project. Besides, in chapter 1 the research aim and the objective is defined. In chapter 2, a theoretical background is given, to elaborate the principles and aspects present in this research. Next, in chapter 3 the materials and methods used to answer the research questions are extensively described. Finally, in chapter 4 the results will be displayed and discussed, followed by a conclusion and recommendations about potential further research in chapter 5.

2. Theoretical background

First, an introduction to the theorem and the principles of the used positioning methodology is given. Secondly, the method of photogrammetry is explained extensively, in order to describe the process of the retrieval of a DEM from aerial images and measured positions of GCPs.

2.1 Positioning systems

2.1.1 GNSS receivers

As mentioned in the introduction, two types of GNSS devices are used in this research to perform the necessary measurements. Global Navigation Satellite System is the general name for the system of satellites, which are capable of sending signals to GNSS receivers in order to determine the receiver's location (European GNSS Agency, 2017). This is done by measuring the time differences between the received transmissions of the different satellites (Xu, 2012). The principle of measuring information from an object or surface, without touching the object or surface, is called 'remote sensing'. Such measurements can be performed by using satellites, but also by using aerial vehicles such as airplanes or drones. The use of the latter will be further elaborated later in this report. The most well-known GNSS are the Global Positioning System (GPS) from the USA, Galileo from Europe, GLONASS from Russia and BeiDou from China. The two particular GNSS devices used in this research are described in the next chapter. Both will do the measurements based on the real-time kinematic (RTK) technology. This technology enables measurements on centimetre level to be done without post-processing the data (Unavco, 2012). For the RTK technique, two receivers are needed. The first is the 'base', the reference station, which is static and its position is exactly known. The base broadcasts raw GNSS observations to the 'rover', the other receiver, which is the mobile, "roving" device. The rover is used to measure the positions of the GCPs and to receive correctional information from the base station (Pirti, Yucel, & Gumus, 2013; Xu, 2012). There can only be one base, which is to be placed within a reach of approximately five kilometres from the study area, but a high number of rovers can be used (Unavco, 2012).

2.1.2 Height determination

In this research, the measured heights of the GCPs are most relevant. Further elaboration on the technique behind GNSS receivers lies beyond the scope of this report. The determination of the measured heights, however, is a point of attention. GNSS receivers measure the height relative to a reference ellipsoid, which is a mathematical approximated representation of the physical Earth (Fotopoulos, 2003). The Geodetic Reference System 1980 (GRS80) ellipsoid is the most well-known global reference ellipsoid worldwide, because nowadays most countries use the same, global reference system. In DEMs, elevations are shown as a distance relatively to a reference surface, to which is referred as the orthometric height (Unavco, 2012). The reference surface is in most cases the global sea level and is called the reference geoid, because this equipotential surface of the Earth's gravity is said to be the best approximation of the mean sea level (Fotopoulos, 2003). The reference geoid has been modelled in several global or regional models, the most widely used is the Earth Gravitational Model 1996 (EGM96) geoid. For the Netherlands in particular, specific (quasi-)geoid models such as the NLGEO2018 are developed. The geoid height is dependent on the specific position on earth of the measured surface and can be derived from geoid models such as the EGM96. The relation between the geoid, ellipsoidal and orthometric height is shown in Figure 2.1. The green (upper) line is the surface of the particular studied terrain, whereas the smooth reference ellipsoid is described by the red (lower) line and the reference geoid by the blue line in the middle. The GNSS device provides the surface elevation

values relative to a reference ellipsoid. So, if the elevation relative to the reference geoid – known as the topographic or orthometric height – is to be known, the geoid height can be subtracted from the ellipsoidal height. In the Netherlands the orthometric height is usually given relative to NAP (Normaal Amsterdams Peil), the Dutch reference height.

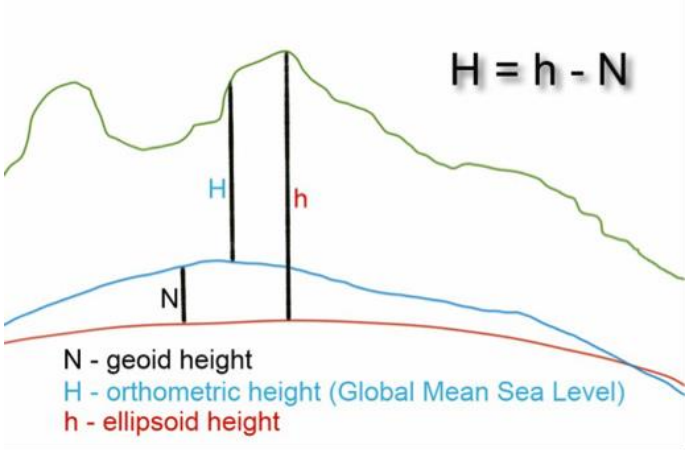

Figure 2.1: relation between height terms (Unavco, 2019).

2.1.3 Coordinate systems

Another important aspect of the performed measurements, is the coordinate reference system that is used. Coordinates can be ECEF (Earth-Centered, Earth-Fixed) where positions are represented by X, Y, Z coordinates, or they can be geographical (geodetic), where positions are represented in longitude, latitude and elevation (Van der Marel, H., personal communication, 2020). All coordinates that are measured, are given with respect to a certain reference system. The reference systems are described by the International Terrestrial Reference System (ITRS), of which the European Terrestrial Reference System 1989 (ETRS89) is the European realization. ITRS is realised by scientific institutes and universities. ETRS89 is the only geodetic datum to be used in Europe, and is based on the GRS80 ellipsoid. The European Terrestrial Reference Frame 2000 (ETRF2000) is a specific, local solution of the ETRS89. The ETRF2000 is used for the measurements in this report. GPS systems use the World Geodetic System 1984 (WGS84) for cartography and geodesy purposes as the standard. WGS84 was developed by the US National Geospatial-Intelligence Agency in 1984 and describes for instance the used coordinate system and the used reference ellipsoid. The WGS84 is based on the ITRS. Originally, the WGS84 used the GRS80 ellipsoid, but it now uses its own refined reference ellipsoid. The differences between the GRS80 and WGS84 ellipsoids, however, appear to be smaller than millimetres.

2.2 Photogrammetry for DEMs

2.2.1 Methodology

In order to compose an elevation map from UAV images and known positions of measured GCPs, a particular method called photogrammetry is used. Photogrammetry can be seen as the “discipline of extracting metric information from photographs”, as described by Tiberius, Van Leijen, and Mousivand (2017, p. 11). Obtaining topographic information from aerial images is the most widely used specific application of photogrammetry. This method describes the processing phase from information derived from 2D aerial images to the construction of 3D models such as a DEM. It can be performed by photogrammetric software, with the aerial photographs and self-measured GCPs as input data. According to Balogh and Kiss (2014), photographs taken by aerial vehicles always result in optically distorted images because every image is taken from a (slightly) different altitude or angle. Such

geometrical errors in images are caused by the optics of the camera, which means the type and the settings of the camera lens, or by the tilt of the camera and in which way it was directed. More tilted photographs result in more distorted images. In addition, the topographic relief in the studied terrain plays a role, as shown in Figure 2.2. In this figure it is visible how the altitudes of the points on the surface of the terrain are adjusted to the projection plane by the camera, which results in the distortion of the photographs (Balogh and Kiss, 2014).

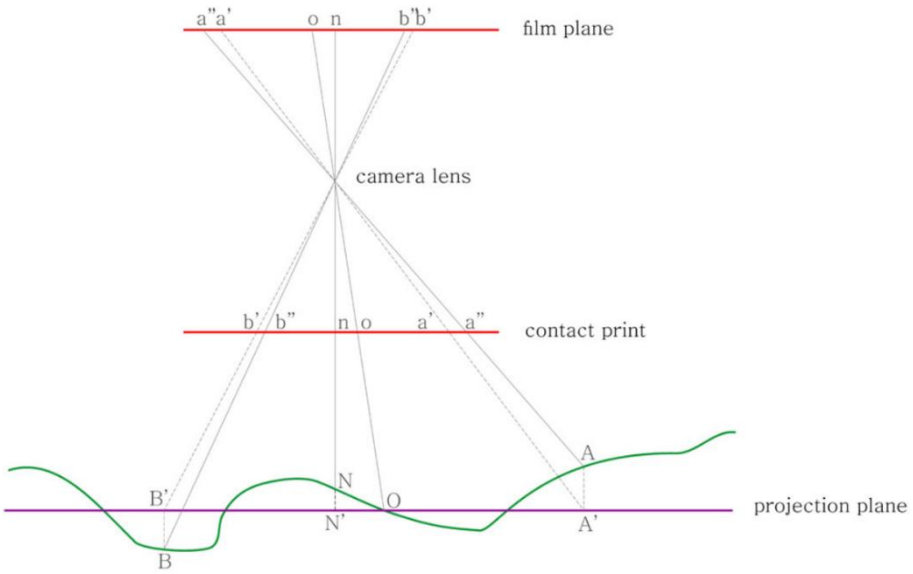

Figure 2.2: geometrical distortion of images due to topographic relief. (Balogh and Kiss, 2014).

In order to derive geometric information from such images, calibration of the camera is necessary. Intrinsic parameters such as the focal length and the centre of the image are to be determined or estimated, in order to correct the images for lens distortion or to measure the size of a captured object (Tiberius et al., 2017). This covers the interior orientation of the photograph. For the exterior orientation, firstly, the terrain and the camera coordinates need to be in the same terrestrial coordinate system. Explanation on those coordinate systems is given in paragraph 2.1.3. The photographs need to be georectified, which means putting an image from its original geometry into a certain map projection (ImagerySpeaks, 2012). The camera coordinates can be transformed into the terrain coordinates through a three dimensional similarity transformation, in which translation, rotation and scale describe relations between coordinate systems (Van der Marel, 2020, p. 17). This means that always a certain coordinate system is to be used as a starting point, so for example the origin of the terrain coordinate system can be taken. As shown in Figure 2.3, with C the centre of the camera, three rotations (ω, φ, and κ) and a translation over vector (X_C, Y_C, Z_C) are performed for the transformation. Then, after scaling, the point P of the terrain is depicted at the camera coordinates x_P, y_P.

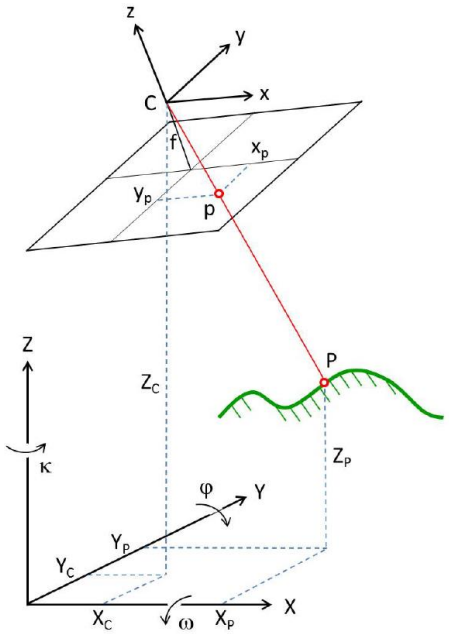

Figure 2.3: transformation between terrain and camera coordinate systems (Tiberius et al., 2017).

For the external part of the camera calibration, the position of the camera centre and the orientation of the camera relative to the study terrain are taken into account as well. During the caption of the images, the position and orientation are unknown. In order to retrieve accurate maps, consequently, geometric corrections of the aerial images are needed. This can be done by measuring the position and orientation of the camera during the flight, or, as applied in this research, by known information of the exact positions – in the desired coordinate system – of determined GCPs in the area. These positions are to be measured with GNSS devices prior to the imagery phase, to ensure that the exact coordinates are known before the images are captured. Only then, the position and orientation of the camera can be reconstructed. Therefore it is important to use markers for the GCPs in order to make them visible for the aerial camera. Moreover, it is useful to measure a redundant number of GCPs to make sure enough information is obtained in case unusable GCPs occur. The more (and the more accurate) GCPs are used in the photogrammetric correction, the more accurate the generated 3D model will be (Van Til, J., personal communication, 2020). Without the use of GCPs, 3D models such as elevation maps tend to get the shape of a bowl, which may result in inaccurate elevation values. The reason for this is the fact that the edges of the 3D models are based on less camera positions, because at the edges less surrounding images of the particular surface points are captured.

To be able to construct a high resolution 3D model from the aerial images, sufficient overlap of the photographs is needed in order to capture every image from a different position and viewpoint (Balogh and Kiss, 2014), as shown in Figure 2.4. In case of a UAV as the aerial vehicle, this can be programmed by the pilot by setting up a so-called waypoint flight, in which the desired area is determined and the autopilot of the UAV consequently plots the flight route including the overlap automatically. Only by using two or more images of the same object or surface, a three dimensional model of this object or surface can be retrieved. The same points need to be seen from different angles. This method is called stereo photogrammetry, where captured, overlapping aerial photographs are merged together to create a set of images on which common points can be matched.

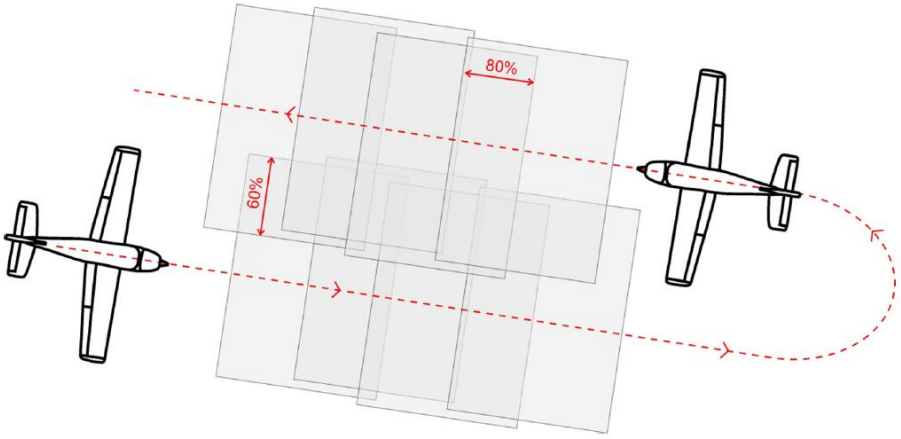

Figure 2.4: overlap between aerial images (Balogh and Kiss, 2014).

2.2.2 Processing phase

In the next phase, after the photographs are captured by the aerial camera, the images and the related data are put into modelling programs to create a 3D model. This process can be done by photogrammetric software such as Agisoft Photoscan or OpenDroneMap. In this research, Agisoft Photoscan is used. The software can obtain metric information from every single image such as the height of visible objects by using its knowledge of the flying height and the positions of object bottoms and tops. The position and orientation of the camera must be known for the software to derive such information. After the photographs are imported and sorted in the software, certain undesired or unnecessary images or details on the images can be masked to remove low-quality, moving or shiny areas from the process and from the calculations. Then, as described in the previous paragraph, feature points on the images can be detected and matched by matching algorithms such as Scale-Invariant Feature Transform (SIFT) and Structure-from-Motion (SfM) (Westoby, Brasington, Glasser, Hambrey, & Reynolds, 2012), which use multiple, overlapping images to extract information (Figure 2.5).

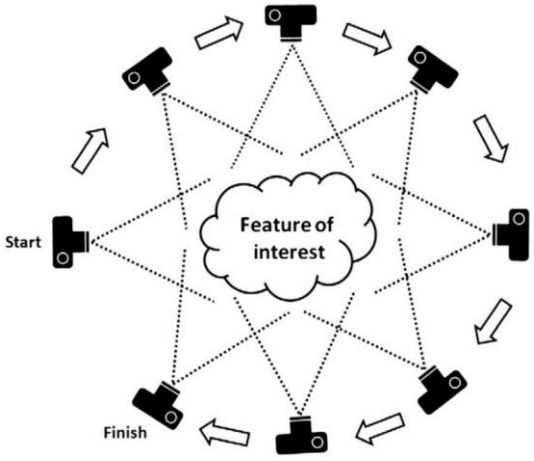

Figure 2.5: the SfM algorithm uses multiple, overlapping photographs (Westoby et al., 2012).

Algorithms like Structure-from-Motion are capable of calculating matching points along with the corresponding camera positions and orientations and the previously mentioned intrinsic camera parameters. The position and orientation together are referred to as the pose of a camera. From the position of the camera a line of sight can be constructed to a certain captured object or point, resulting in numerous lines from which the intersection determines the three-dimensional location of the object or point. This process is called triangulation. From this information, a sparse point cloud is generated,

which gives a rough representation of the original shapes of captured objects. Consequently, an enhanced, denser point cloud is retrieved, based on the output of the sparse point cloud. In this stage, the measured GCPs are added to the software to georectify the model (as described in the previous paragraph). Also, the projection system is determined. Finally, a 3D dense point cloud can be reconstructed by the implementation of multi-view stereo (MVS) algorithms, which uses the camera pose from the sparse point cloud along with the geometric information from the GCPs (Furukawa, Curless, Seitz, & Szeliski, 2010). It results in depth maps on which the distances from the images to certain reference points are represented. From the dense point cloud, it might be necessary to remove outliers. Afterwards, based on the dense point cloud, a polygonal mesh is built for geometry, which represents the surfaces of the objects. The mesh can then be textured using the original images. As a result, DEMs and orthomosaic photos (orthophotos) can be created. An orthophoto is an aerial photo constructed from captured aerial images and geometrically corrected for lens distortion, topographic relief and camera tilt, so it is an accurate representation of an area. It is needed in the case of a DEM analysis as a background image with the same accuracy as a map. An overview of the whole generation process is shown schematically in Figure 2.6. Eventually, geo-informatic analyses can be performed in software programs such as QGIS (Quantum Geographic Information System).

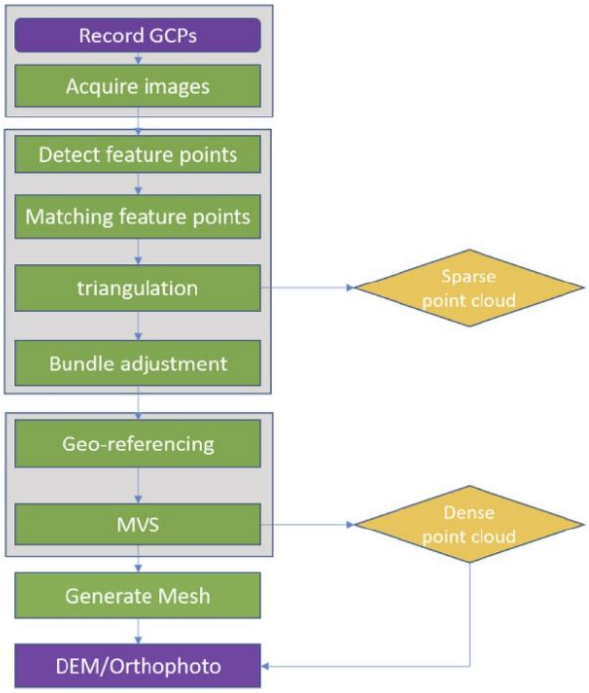

Figure 2.6: photogrammetry process to DEM (Samboko et al., 2020).

3. Materials and methods

First, the total number and the specific locations of the GCPs within the chosen study area are determined. The positions of the GCPs are measured by both the low-cost and the professional GNSS receiver. Subsequently, the UAV will capture images of the terrain including the GCPs clearly visible. Finally, the exact measured positions of the GCPs by the two receivers will be used separately, both combined with the UAV images along with any camera information or calibration, as input to create two separate DEMs per device. The images from the UAV are corrected by the position information from the GCPs, as described in the previous chapter about photogrammetry. Afterwards, the differences in accuracy of the results can be analysed and discussed. In this chapter, both the low-cost and professional alternative are explained. Moreover, the used UAV and the requirements of the study area are described, along with a brief description of the measure plan. Finally, the processing phase of the data and the analysis of the retrieved results are explained. Below, in Figure 3.1, the research including the test scenarios is represented in a schematic overview, which will be elaborated in this chapter.

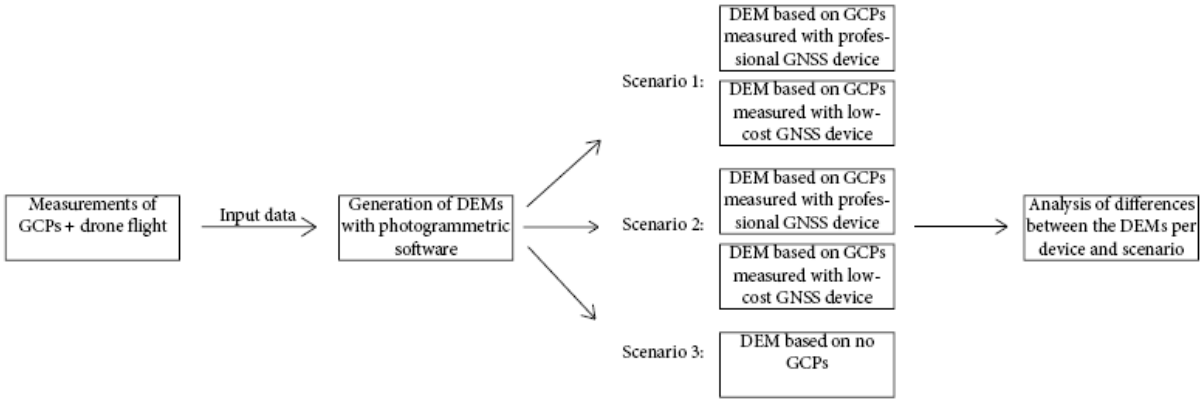

Figure 3.1: flow chart of the research.

3.1 Low-cost GNSS receiver

The low-cost receiver exists of an inner UBlox device and an outer 3D-printed design. The inside is provided, and under research, by Andreas Krietemeyer, PhD researcher at the TU Delft, department of Water Resources Management. His research focuses on improving localized extreme rainfall forecast models using low-cost GNSS receivers (TU Delft, n.d.). The equipment layout of the receiver is designed by Peter Verweij, graduate student in Industrial Design Engineering at the TU Delft, as can be seen in Figures 3.2 and 3.3. The UBlox antenna is constructed on top and the whole prototype can be placed on a tripod.

In order to perform measurements with the low-cost receiver, a base station and a rover are needed, as described in paragraph 2.1. The base station is static and its position is exactly known. Tests can then be done by using the rover to measure the x, y and z-coordinates with respect to the coordinates of the base station. The base station is slightly different from the rover in its design. At the time of the performed measurements for this report, the exterior design for the base station was not yet finished, but the antenna could be used. The low-cost rover device works with a smartphone as the control unit using Bluetooth. The measurements can be checked in the application 'SW Maps', which is only compatible for Android smartphones. In this application, the GCPs can be measured by recording features while making sure a Fix RTK status for the satellites is active, which is the most accurate status. All the actual information about the number of available satellites and the RTK status can be seen in the application

and connections between the rover and base station can be made quickly. The derived data used for the generation of the DEMs was measured by the 'record feature' option in the application, so the positions were measured in one take. No averaging of ten-second measurements was included. All measurements were performed with a Fix RTK status. Since the position of the low-cost base station was measured by the Trimble device, as explained in Appendix A, the coordinate reference frame for the UBlox data is ETRF2000, as this is the reference frame for the Trimble.

Figure 3.2 and 3.3: design of the exterior of the low-cost device prototype (Peter Verweij, 2020).

3.2 Professional Trimble R8 device

The professional, high priced receiver that will be used in this research is the Trimble R8. This device belongs to the TU Delft, department of Geosciences and Remote Sensing (contact is Hans van der Marel). The Trimble R8 (see Figures 3.4 and 3.5) is capable of performing RTK measurements of ground control points without the need of a base station close by, which is the method used in this research. This method "requires a real-time data link with a service provider", according to Van der Marel (2019, p. 3). In this case, the NETPOS (Netherlands Positioning Service) from the Dutch Kadaster is used. This is a network of GNSS reference (base) stations, distributed over the Netherlands with an in between distance of around 40 kilometres, which results in a good coverage throughout the whole country (Kadaster, n.d.). The main advantage is that no post-processing is needed, the measured coordinates are stored in the data collector of the R8 itself. The measured coordinates are, as well as the UBlox data, in the ETRF2000 frame. The collected data will be processed by Hans van der Marel and will be discussed in this report.

Figure 3.4 and 3.5: Trimble R8 antenna and equipment (720i (2020), precision-geosystems (2017)).

3.3 UAV imagery

In order to retrieve UAV images needed for the construction of a DEM, a drone from HiView is used. HiView is a company with expertise in projects where UAV imagery is involved and offers a lot of experience with drone flights. Our contact and pilot is Jan van Til, operational manager at HiView and experienced drone pilot, who will manage the drone flight over the study area during the research. The used drone is the eBee Classic by SenseFly, a Swiss drone company. Figure 3.6 shows Jan van Til during the launch of the drone flight. The drone flew at a height of 114.5 meter during our flight day and a regular, standard RGB (red, green and blue light) camera was used. The images were taken nadir, which means 100% vertically pointed, and at specific time intervals. In order to achieve sufficient overlap, necessary for proper DEM generation as described in paragraph 2.2 on photogrammetry, a waypoint flight was programmed on Jan's computer. "During a waypoint flight the plane is controlled by the autopilot on a pre-set route and altitude", according to Balogh and Kiss (2014, p. 2). The flight altitude was also programmed in this waypoint flight. The GCPs need to be visible for the UAV and were therefore marked with large blue bags, as can be seen in Figure 3.7. During the flight, 214 images from different positions were taken to cover the study area.

Figure 3.6: Jan van Til with the UAV.

Figure 3.7: visible marker point of a GCP.

3.4 Study area

3.4.1 Location

A few important aspects such as height difference and vegetation were taken into consideration in the study to an appropriate area. The area to be studied needs to have a range of 15-30 hectares, according to Jan van Til, in order to be able to create a proper informative DEM. The area should not contain a lot of water as well, as this can result in blinking and therefore unusable images captured by the UAV. A study was done to potential areas, which resulted in the following location: nature reserve the Breemwaard, a floodplain between the villages Zuilichem and Nieuwaal in Gelderland, The Netherlands. Permission to fly with a UAV was granted at the Dutch Air Traffic Control and Staatsbosbeheer, owner of the area.

3.4.2 Measure plan

Regarding the GCPs, Jan van Til recommended to stick to a maximum of 250 meters between the points which mark the GCPs. In addition, at least 10 GCPs were required to generate a sufficiently informative DEM. Because of the research questions about the number and the spatial distribution of the GCPs and due to the fact that each point has to be measured twice (low-cost and professional), preparations for approximately 40 total measurements were made. Eventually, 19 markers for GCPs were placed within

an area of 27 hectares and were measured (twice). In order to answer the questions, certain GCPs are left out in the processing phase to monitor its effect on the accuracy of a generated DEM. The specific study area is shown in Figure 3.8, along with an overview of the positions of the measured GCPs. For further elaboration on the planning of the measurements, see Appendix A for the measure plan as a whole.

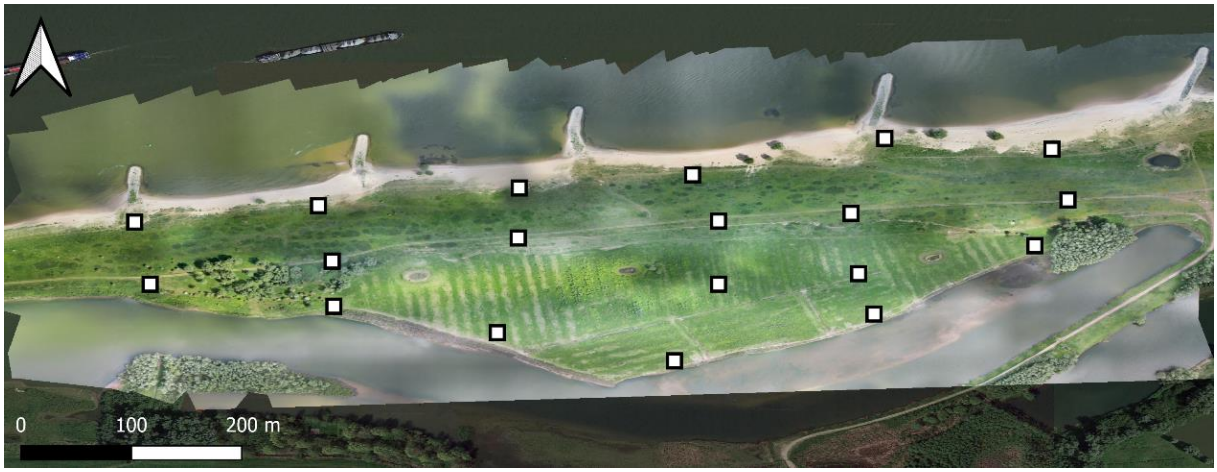

Figure 3.8: the study area 'Breemwaard' including the measured GCPs (QGIS export).

3.5 Data processing

3.5.1 DEM generation

After the measurements and the UAV flight were finished, the processing phase of the elevation maps was performed by Jan van Til from HiView. The measured data from the UBlox and the Trimble R8 devices were sent to Jan and along with the UAV images covering the 27 hectares study area, which were geotagged by Jan, the desired DEMs and orthomosaic photos were generated in Agisoft Photoscan Professional. Geotagging means that to every pixel in the captured images a coordinate was assigned. The images were geotagged in WGS84, the geodetic system which is described in paragraph 2.1.3. The DEMs have a resolution of approximately 7.3x7.3cm and the orthophotos have a resolution of approximately 3.6x3.6cm.

A further study to the differences in accuracy between the Trimble R8 and the UBlox receivers in horizontal and vertical alignment is done by Ivo van Balen, fellow BSc student Civil Engineering at TU Delft. From that research, it can be checked if measured values by the UBlox compare favourably with the Trimble R8 values. If so, the GCPs for generating a DEM measured by the UBlox device can be assumed accurate.

3.5.2 Results analysis

The goal of the research is to find out if certain factors regarding the use of GCPs in the processing phase influence the accuracy of the final DEM. This is described in paragraph 1.2 and elaborated furtherly in Appendix B. Therefore, three scenarios of DEMs were processed by Jan van Til, as described below:

- Scenario 1: all measured GCPs were used in the DEM generation process, which result in a dense network of GCPs;
- Scenario 2: only four of the measured GCPs on the edges of the study area were used in the DEM generation process, so this scenario represents a sparse network of GCPs (see Figure 3.9);

- Scenario 3: none of the measured GCPs were used in the DEM generation process, so no corrections by GCPs could be made. Only internal positioning and orientation sensors were used.

Figure 3.9: study area in scenario 2, only four GCPs taken into account (QGIS export).

By setting up the different scenarios, the effects of a dense, sparse and absent network of GCPs on the accuracy of a generated DEM can be researched. Consequently, the optimal number of necessary GCPs is taken into consideration. The DEM derived from the Trimble R8 in scenario 1 is used as the reference DEM. In order to analyse the derived elevation maps, the software of geographic information system QGIS 3.12 Bucuresti was used. The WGS84 was used as the geodetic system in QGIS. Using the derived DEM for each scenario separately, the elevation values at 54 random positions (flat and free from vegetation) spread over the study area were compared and analysed. The differences between the DEMs, along with the mean absolute error (MAE) and the root mean squared error (RMSE), were monitored for each position, for each scenario. It is important that the chosen positions are interpolated points – so, surrounding the positions of the GCPs – which are constructed by the photogrammetric software itself. This way, the influence of the circumstances per scenario on the accuracy of a DEM can be seen, assuming that the DEMs derived from the Trimble data are accurate. Besides, the influences are checked for both the Trimble and UBlox DEMs, from which the usability of the UBlox device in generating a DEM can be evaluated. Finally, recommendations can be made on achieving an as accurate as possible DEM with a UBlox device. The results are presented and discussed in the following chapter.

4. Results and discussion

4.1 Retrieved products

As described in the previous chapter, the elevation values from the retrieved DEMs for each scenario were compared in QGIS. Per scenario, a DEM and orthophoto for both the Trimble and UBlox data were generated. In Figure 4.1, an orthophoto is shown, which is an accurate representation of the study area captured by the camera of the UAV, as described in paragraph 2.2.2. This orthophoto in particular was generated for scenario 1 by using all measured GCPs from the Trimble data. The other generated orthophotos differ slightly, but not clearly visibly from the presented one. In the orthophoto it can clearly be seen that the study area lies slightly more in the lower half of the captured terrain by the UAV camera. The same goes for the DEMs.

Below, the retrieved DEMs for scenario 1 (Trimble R8) and for scenario 3 are presented as well (Figures 4.2 and 4.3). The other DEMs are presented in Appendix C. In each DEM it can be seen that some low and high elevation values occur, with the lowest values representing the water surfaces and the highest values representing the vegetation, most of it being large trees. The visible differences between the DEMs from scenario 1 and 2 mostly occur on the edges of the maps or on vegetation (the white parts). The reason for this is the manual removal of the outliers in the dense point cloud, which is carried out slightly differently per scenario. The DEM from scenario 3, however, clearly shows a different representation of the area than the other scenarios do. This can also be seen in the accuracy results discussed in the next paragraph.

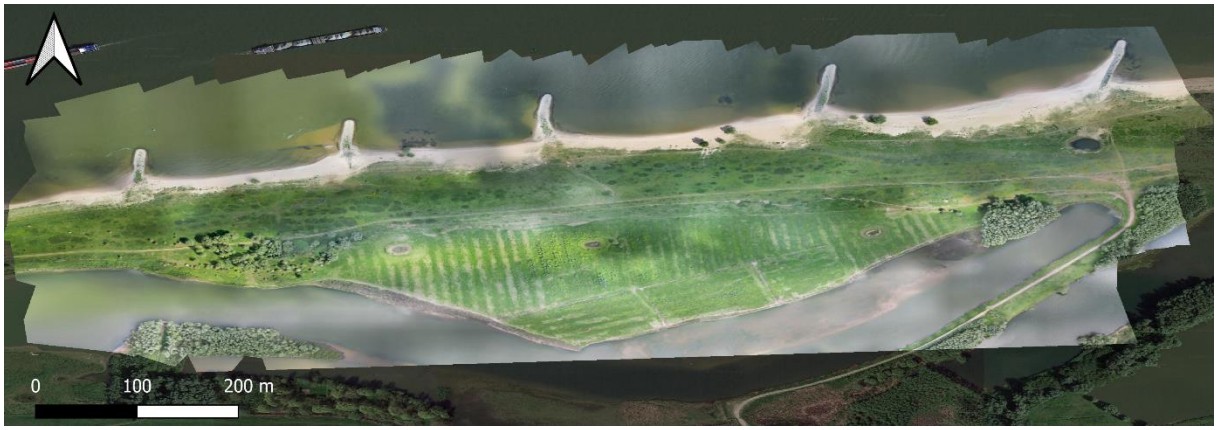

Figure 4.1: orthomosaic photo of the study area with Google Satellite as background (QGIS export).

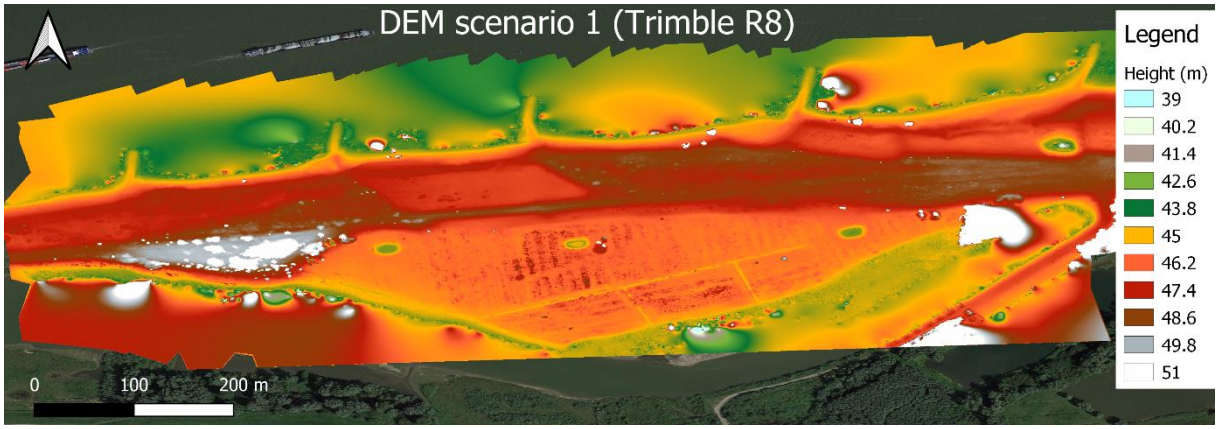

Figure 4.2: DEM in scenario 1 from the Trimble R8 data, generated with the use of 19 GCPs.

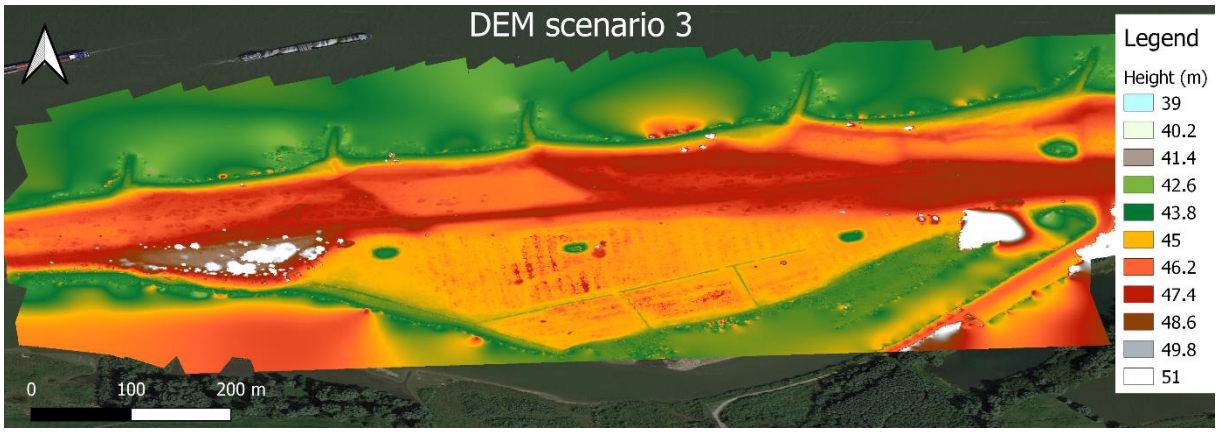

Figure 4.3: DEM in scenario 3, generated without the use of GCPs.

4.2 Analysed results

4.2.1 UBlox to reference DEM

In Table 4.1 an overview is given of the elevation errors of the three DEMs generated with the UBlox data, relative to the reference DEM. As described in paragraph 3.5.2, the DEM based on Trimble R8 data in scenario 1 (19 GCPs) is used as the reference DEM. For the UBlox DEMs, each scenario is analysed with respect to the reference DEM. The maximum positive and negative errors are calculated, as well as the mean absolute error (MAE) and the root mean squared error (RMSE). The RMSE increases when larger errors occur, so if larger errors are significantly more undesired than smaller errors, the RMSE is useful to look at. If the size of the error is not important, the MAE is more appropriate to use.

The most important result the table shows, is the small difference between the errors with 19 GCPs and 4 GCPs (scenario 1 and 2). The coverage of GCPs per hectare in the scenario with 4 GCPs is significantly lower with a factor of 4.75, whilst the MAE and RMSE only increase with a factor of 1.82 and 1.71, respectively. This can mean that for some applications requiring low accuracy elevation data, instead of a dense GCP network, only few GCPs are needed to create a usable DEM.

	Number of GCPs		
	19	**4**	**0**
GCPs per hectare	0.70	0.15	0
Max positive elevation error	0.023434	0.082984	- (min negative: -0.567155)
Max negative elevation error	-0.06694	-0.116683	-1.011213
Mean absolute elevation error	0.017685333	0.032217741	0.765333463
Root mean squared error	0.023914998	0.040827899	0.773785578

Table 4.1: accuracy of DEMs based on UBlox data relative to reference DEM.

In scenario 3 (0 GCPs), however, the errors occur to be much larger. The MAE and RSME increase with factors 43.28 and 32.36 with respect to scenario 1 with 19 GCPs. Moreover, all elevation values are lower than in the reference DEM. The errors range from approximately 0.50 to 1.00 metres, which could indicate a constant negative deviation or bias, but the errors vary too widely to determine a specific bias.

The large errors were not unexpected for this scenario where only the internal GPS of the UAV flying sensor calculates the elevations for the DEM, since it is known from previous researches that UAVs use simple GPS and inertial measurements (IMU) sensors which are not capable of "producing usable DEM data in the absence of external GNSS reference data" (Coveney & Roberts, 2017, p. 18 (3175)). The distortion in the aerial images, as discussed in paragraph 2.2, is corrected by the use of GCPs in the generation process of a DEM. If no GCPs are used to correct the distorted DEM, the elevation map tends to get the shape of a bowl, which may result in inaccurate elevation values.

4.2.2 Location dependence

As mentioned in paragraph 3.5.2, the analysis is based on 54 points spread over the study area. The chosen points are interpolated points of the DEM, which are constructed by the photogrammetric software itself. Figure 4.4 shows the spatial positions of the studied points. Figures 4.5 and 4.6 show the distribution of the elevation errors per point. In Appendix D, all elevation values per studied point are displayed in tables.

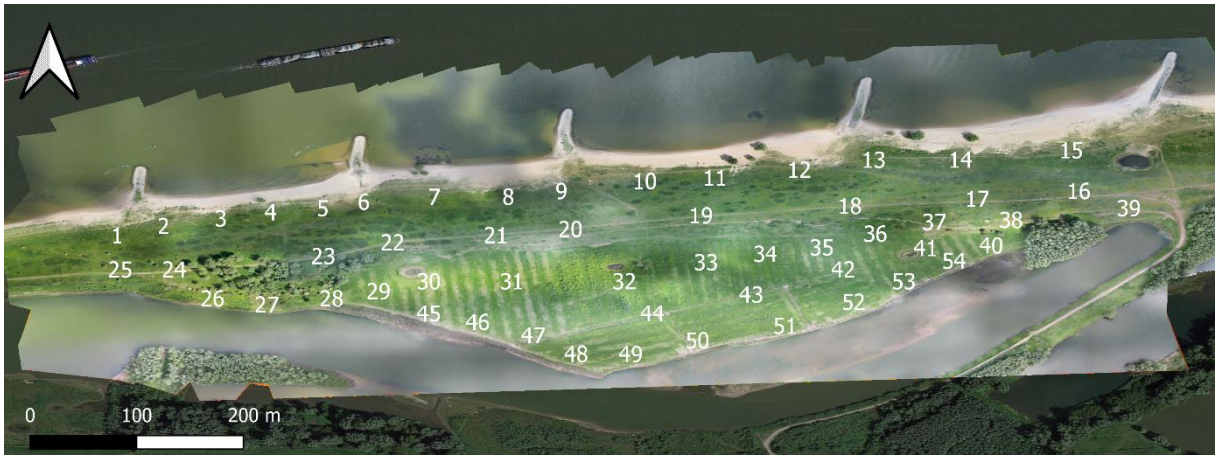

Figure 4.4: spatial distribution of the studied points in the study area.

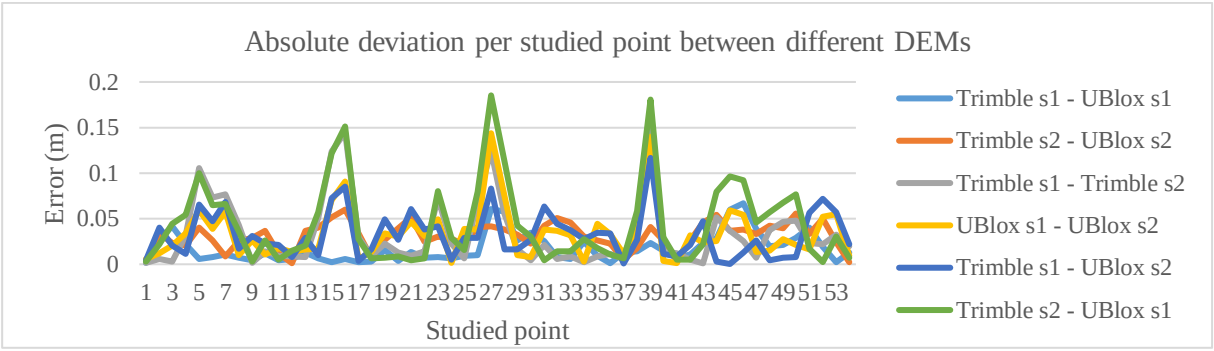

Figure 4.5: absolute deviations between the derived DEMs in scenario 1 and 2 per studied point.

Analysing the spatial positions of the points in combination with the corresponding elevation values, it can be said that the errors are larger at the edges of the model for all DEMs in all scenarios. This is visually presented in Figure 4.4 and Figure 4.5. It can be seen from the points on the edges 15, 16, 27, and 39, and in most cases also points 5, 28, 44-46, 50, and 52, where large errors occur. This is an expected result, due to the previously described fact (paragraph 2.2) that 3D models based on aerial images tend to shape like a bowl, resulting in inaccurate elevation values at the edges. It is clearly visible that the errors at the edges of the map generally increase relatively more in scenario 2. This might be a logical appearance as well, because the less GCPs used in the generation phase, the more distorted the map will be. That's why, as already introduced in the previous paragraph, the errors are extremely large

in scenario 3. This is clearly visible at the edges of the map (points 1-6, 9, 15, 24, 25, and 27), as can be derived from Figure 4.4 and 4.6.

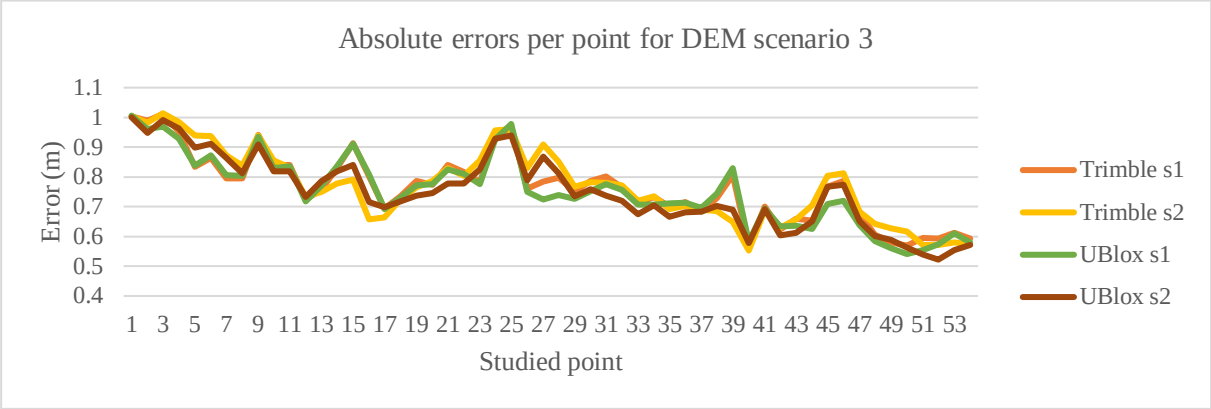

Figure 4.6: absolute errors per studied point for DEM in scenario 3 relative to the other DEMs.

Overall, it is visible that the errors of the points in the upper half of the model are significantly lower than in the lower half. The reason for this can be the fact that the chosen points in the lower half are quite close to the lower edge of the map, whilst the upper half of the chosen points largely lies in the middle of the DEM.

4.2.3 DEM comparison UBlox – Trimble

In addition to the analysis of the UBlox DEMs relative to the reference DEM, other comparisons between all of the other derived DEMs were made. The results of this analysis are displayed in Appendix E. From these results, it can be stated that the performances of the UBlox compare favourably with the Trimble R8. This means that for most applications where some space is available for small inaccuracies up to a few centimetres, the UBlox receiver is a good alternative to the Trimble R8. Next to that, these results also confirmed the expectation that the more GCPs are used, the more accurate the DEM will be. The DEM generated in scenario 1 (19 GCPs) with the UBlox results in more accurate results than the DEM generated in scenario 2 (four GCPs) with the Trimble R8.

4.2.4 Accuracy GCPs – interpolated points

Assuming that the elevation values at the specific positions of the GCPs, used for correction of the DEM, are of a higher accuracy than at interpolated points, only the latter were analysed. The elevation values of the GCPs, however, were taken into account additionally, as shown in Appendix F. These results show that, overall, the errors of the interpolated points are actually similar with the errors of the 19 GCPs. Only the maximum positive and negative errors seem to be considerably lower for the positions of the GCPs. It is also clearly visible that the MAE and RMSE on the positions of the GCPs increase in scenario 2 with respect to scenario 1 and even become larger than the MAE and RMSE of the interpolated points. This can be caused by the fact that scenario 2 uses only four of the GCPs to be corrected with, resulting in more points to be interpolated by the photogrammetric software.

4.3 Discussion

4.3.1 Possible error reasons

As mentioned in the previous paragraph, the errors between the DEMs from the different scenarios and the reference DEM vary per studied position in the area. The reason for this is the original distortion of the aerial images, which are corrected by including the coordinates of the GCPs in the DEM generation

process. At the edges of the models, less positions of the camera are available. In the different scenarios, different numbers of GCPs are used in this process, which clearly resulted in different distortions of the DEMs. The consequence of this may be that some of the elevation values on the studied positions are not representative or realistic. This may have led to some unrealistic errors in the performed analyses.

Other possible causes for the occurrence of errors might be erroneous measurements of the GCPs during the field days. When the receiver is not put in the soil precisely and mindfully, errors of millimetres or sometimes centimetres can occur quickly. Next to that, minor deviations occur between the different orthomosaic images. For the analysis of the different DEMs in QGIS, the orthophoto of the reference DEM (Trimble R8 in scenario 1) is used to locate the positions of the studied points. If the orthophoto, and thus the DEM of one of the other scenarios differs from the reference orthophoto, errors in the elevation values can arise. The maximum horizontal deviation between the orthophotos that can occur, however, is known to be 5 cm. This is a range within the study area in which the elevation values of the DEM did not seem to vary significantly, so this phenomenon will not result in large errors.

Lastly, the photogrammetric software of Agisoft Photoscan could have played a role in some remarkable results. As can be seen in Appendix E, the comparison between the Trimble DEM in scenario 1 and the UBlox DEM in scenario 2 resulted in higher errors than the comparison between the Trimble DEM in scenario 2 and the UBlox DEM in scenario 2. A reason for this can be that the software uses other methods or assumptions when using a lower number of GCPs. This might have led to erroneous elevation values in other scenarios as well.

4.3.2 User dependence

One of the goals of this research is to find the optimal number of GCPs that is needed per hectare, in order to retrieve a sufficiently accurate and usable DEM. The desired accuracy highly depends on the application and the final purpose of the generated DEM. Some users of elevation maps benefit more from having affordable equipment than from having extremely accurate – and thus probably high priced – models. For instance, most users such as agricultural producers or building companies from the regions of sub-Saharan Africa, as described in paragraph 1.1, need representations of the surface of the terrain of interest. In these cases, errors lower than 3 cm may not declare the models unusable for them. On the other hand, some applications such as flood modelling demand high accuracy maps, as “even relatively small DEM elevation errors can result in substantially erroneous predictions of potential horizontal flood in shallow-gradient contexts” (Coveney & Roberts, 2017, p. 12 (3169)). From the derived results it is seen that using more GCPs result in more accurate DEMs. Consequently, it can be said that the number of necessary GCPs depend on the final purpose of the DEM.

5. Conclusions and recommendations

5.1 Conclusions

This research studied the method of retrieving a DEM from UAV imagery and GCPs collected by a low-cost positioning device. In addition, the effect of the number, distance and spatial distribution of the GCPs on the accuracy of a DEM were taken into account in order to answer the research sub-questions as formulated in Chapter 1.

It is found that by determining an appropriate study area, measuring the positions of reference GCPs in this area and consecutively mapping the area with a UAV to retrieve aerial images from different angles and positions, a DEM can be generated by photogrammetric software. The captured aerial images are matched together in a model, which then needs to be corrected by the exact positions of the GCPs in order to obtain a 3D model that is not distorted. Through varying the number of measured GCPs in the generation of the elevation map, the effects of a dense, sparse and absent network of correctional GCPs on the accuracy of a DEM can be monitored. With this analysis, the main research question was answered:

"What accuracy of an elevation model can be achieved if it is retrieved using ground control points collected by a low-cost positioning device?"

An elevation model retrieved by a low-cost positioning device and a dense network of GCPs to correct the UAV images resulted in a mean absolute error and root mean squared error of approximately 1.77 and 2.39 centimetres, respectively. The errors were measured relative to a DEM generated by a professional GNSS receiver using a dense network of GCPs, which was set to be the reference DEM. The second elevation map retrieved by using a low-cost receiver, but then corrected by a sparse network of GCPs (number of GCPs decreased with factor 4.75) with GCPs only on the corners of the area, resulted in a mean absolute error and root mean squared error of approximately 3.22 and 4.08 centimetres. So, the errors only increased with a factor of 1.82 and 1.71 relative to the DEM based on a dense network of GCPs. The decision if this accuracy is favourable and sufficiently accurate for the user, is highly dependent on the final application of the elevation model. It can be stated that the acquisition of accurate GCPs is difficult in most study environments due to the high requirements of the measurements – no canopy, structures or vegetation around the measured points are preferred. Therefore, it is often desired that as few as possible GCPs are used for the generation of a DEM. Overall, from other analyses in this research, it can be concluded that the more GCPs are used, the more accurate the DEM will be. The DEM generated with a dense network of GCPs collected by the low-cost receiver results in more accurate results than the DEM generated with a sparse network of GCPs with a professional, high priced GNSS receiver. However, for some purposes, accuracy differences up to 3 centimetres are certainly sufficiently accurate and deliver still usable models. From this, it can be concluded that in some cases, it is more preferable to have a low number of GCPs, provided that small deviations in elevation values will not cause unfavourable events. On the other hand, it can also be concluded from this study that using low-cost derived DEMs for river flood predictions comes with a risk, as it is said that such predictions need high accuracy elevation data.

The third scenario that was analysed in this research, was the generation of a DEM without the use of GCPs. This resulted in a DEM with large errors and a constant negative deviation with respect to the derived DEMs in the other scenarios. It can thus be concluded that the use of no GCPs is not recommended, as using a small number of GCPs already achieves a relatively high accuracy. Furthermore, based on all the results combined, it can be concluded that regardless of the number of GCPs used to correct the model, larger inaccuracies keep present at the edges of the DEMs. In all

scenarios, elevation values near the edges of the model deviated more from each other and the inaccuracies relative to the reference DEM were larger at those positions. The reason for this is the fact that in general, at the edges of a study area, less camera positions are available to capture the terrain. Using a more and more dense network of GCPs to correct the distorted model, the errors do decrease, but will always stay visible.

5.2 Recommendations

The main recommendation of this research is that in studies where acquisition of GCPs is inconvenient and difficult, the use of a small number of GCPs per hectare is highly recommended as this result in considerably higher accuracy than using zero GCPs. Moreover, the accuracy of a DEM based on a few GCPs per hectare compares remarkably favourably with a case in which a high number of GCPs per hectare is used. For purposes regarding flood risk simulation, on the other hand, it is highly recommended to use available flood models to compare the results of the DEMs with. River flood predictions require very high accuracy DEM data. From the comparisons in this research, not much can be said about the usability of the low-cost derived DEMs in flood modelling due to the high risk of disastrous events when errors are made in this process.

Based on this research, it can also be recommended that further research is done to the determination and use of GCPs in generating elevation maps. This report focussed on only three scenarios due to the amount of time that was available, but it can be stated that analysing more different scenarios will lead to more information and thus more complete answers to the research questions of this report. In order to determine the optimal number of GCPs per hectare that is needed to derive accurate models with low effort and costs, it is recommended to research the use of more differing numbers of GCPs within the range of zero to one GCP per hectare. This way, the knowledge of the minimum number of GCPs needed to generate a sufficiently accurate DEM for the desired application is optimized.

Finally, the derived results could be checked more professionally with scientifically derived DEMs, from which more realistic and more scientifically sound conclusions can be made. The DEMs can for instance be referenced to commercial DEMs conducted by large scientific organizations such as US Geological Survey in cooperation with NASA. These DEMs use satellites which are launched specifically for purposes such as the retrieval of global elevation maps. Some other DEMs are constructed using Lidar (Laser Imaging Detection And Ranging) technologies, which is an expensive, but extremely accurate method which could deliver reference DEMs for this study.

In summary, this research gave insight in the research question, however more thorough research on elevation maps in particular applications that require high accuracy elevation data is needed.

References

African Development Bank. (2019). *Feed Africa* [Brochure]. Abidja, Ivory Coast: Author.

Agisoft LLC. (2016). *Agisoft PhotoScan User Manual Professional Edition, Version 1.2*. St. Petersburg, Russia: Author.

Amoateng, P., Finlayson, C. M., Howard, J., & Wilson, B. (2018). A multi-faceted analysis of annual flood incidences in Kumasi, Ghana. *International Journal of Disaster Risk Reduction, 27*, 105-117. doi:10.1016/j.ijdrr.2017.09.044

Balogh, A., & Kiss, K. (2014). Photogrammetric Processing of Aerial Photographs Acquired by UAVs. *Hungarian Archaeology E-journal.* Retrieved from Academia website: https://www.academia.edu/7070293/Photogrammetric_processing_of_aerial_photographs_aquired_by_UAVs

De Boer, F., Van Til, J., Morello, R., & Droogers, P. (2016). *Nulmeting geomorfologische dynamiek stuifzand Hulshorsterzand* (LIFE 10 NAT/NL/000023/actie E3 wuthering heaths). Retrieved from HiView website: https://www.hiview.nl/publications.

Chen, X., Cen, M., Guo, H., Zhang, T., Zhao, C., & Zhang, B. (2018). Chinese satellite photogrammetry without ground control points based on a public DEM using an efficient and robust DEM matching method. *International Journal of Remote Sensing, 39*(3), 704-726. doi:10.1080/01431161.2017.1390270

Coveney, S., & Roberts, K. (2017). Lightweight UAV digital elevation models and orthoimagery for environmental applications: data accuracy evaluation and potential for river flood risk modelling. *International Journal of Remote Sensing, 38*(8-10), 3159-3180. doi:10.1080/01431161.2017.1292074

European GNSS Agency. (2017). What is GNSS?. Retrieved May 6th, 2020, from https://www.gsa.europa.eu/european-gnss/what-gnss

European Union (2014). *HORIZON 2020 in het kort. Het kaderprogramma van de EU voor onderzoek en innovatie.* doi:10.2777/82344

Everaerts, J., Lewyckyj, N., & Fransaer, D. (2004). Pegasus: design of a stratospheric long endurance UAV system for Remote Sensing. *Proceedings of the XXth ISPRS Congress* (pp. 29-33)

Furukawa, Y., Curless, B., Seitz, S.M., & Szeliski, R. (2010). Towards Internet-scale Multi-view Stereo. Retrieved from https://www.microsoft.com/en-us/research/wp-content/uploads/2010/06/Furukawa-CVPR10.pdf

ImagerySpeaks. (2012). Georeferencing vs. Georectification vs. Geocoding. Retrieved May 27th, 2020, from https://imageryspeaks.wordpress.com/2012/01/24/georeferencing-vs-georectification-vs-geocoding/

Van de Giesen, N.C., Krietemeyer, A., Ten Veldhuis, J.A.E., & Annor, F. (2018). TWIGA: Sensors for geo-services in Africa. Early results, perspectives, and an invitation. *Geophysical Research Abstracts, Vol. 20,* EGU2018-10141-1

GISGeography. (2020). DEM, DSM & DTM Differences – A Look at Elevation Models in GIS. Retrieved May 4th, 2020, from https://gisgeography.com/dem-dsm-dtm-differences/

Kadaster. (n.d.). NETPOS. Retrieved May 18th, 2020, from https://zakelijk.kadaster.nl/netpos

Krietemeyer, A., Ten Veldhuis, J.A.E., & Van de Giesen, N.C. (2017). Using Low-Cost GNSS Receivers to Investigate the Small-Scale PrecipitableWater Vapor Variability in the Atmosphere for Improving High Resolution Rainfall Forecasts. *Geophysical Research Abstracts, Vol. 19*, EGU2017-14680

Krietemeyer, A., Ten Veldhuis, J.A.E., Van der Marel, H., Realini, E., & Van de Giesen, N.C. (2018). Potential of Cost-Efficient Single Frequency GNSS Receivers for Water Vapor Monitoring. *Remote Sensing, 10*(9), 1493. doi:10.3390/rs10091493

Krietemeyer, A., Ten Veldhuis, J.A.E., Realini, E., & Van de Giesen, N.C. (2018). Densified GNSS-based water-vapor monitoring network in Rotterdam using low-cost single-frequency receivers. *Geophysical Research Abstracts, Vol. 20*, EGU2018-8961

Van der Marel, H. (2020). *Lecture notes on Reference Systems for Surveying and Mapping*. Delft, The Netherlands: TU Delft.

Van der Marel, H. (2019). *Quick-start guide for the Trimble R8-2 PPK/RTK surveys Version 1.1 (rover)*. Delft, The Netherlands.

OpenDroneMap. (n.d.). WebODM Drone Mapping Software. Retrieved May 5th, 2020, from https://www.opendronemap.org/webodm/

Pirti, A., Yucel, M.A., & Gumus, K. (2013). Testing real time kinematic GNSS (GPS and GPS/Glonass) methods in obstructed and unobstructed sites. *Geodetski vestnik, 57(3):498-512.* Retrieved from ResearchGate website: https://www.researchgate.net/publication/283252209_Testing_real_time_Kinematic_GNSS_GPS_and_GPSGLONASS_methods_in_obstructed_and_unobstructed_sites

Remondino, F., Barazzetti, L., Nex, F., Scaioni, M., & Sarazzi, D. (2011). UAV Photogrammetry For Mapping And 3D Modeling – Current Status And Future Perspectives –. *International Archives of the Photogrammetry, Remote Sensing and Spatial Information Sciences*, Volume XXXVIII-1/C22. doi:10.5194/isprsarchives-XXXVIII-1-C22-25-2011

Rieke, M., Foerster, T., Geipel, J., & Prinz, T. (2011). High-Precision Positioning And Real-Time Data Processing Of Uav-Systems. *International Archives of the Photogrammetry, Remote Sensing and Spatial Information Sciences, Volume XXXVIII-1/C22*. Retrieved from ISPRS website: https://www.isprs.org/publications/archives.aspx

Rock, G., Ries, J.B., & Udelhoven, T. (2011). Sensitivity analysis of UAV-photogrammetry for creating digital elevation models (DEM). *International Archives of the Photogrammetry, Remote Sensing and Spatial Information Sciences, Vol. XXXVIII-1/C22, 69-73*. doi:10.5194/isprsarchives-XXXVIII-1-C22-69-2011

Samboko, H.T., Abas, I., Luxemburg, W.M.J., Savenije, H.H.G., Makurira, H., Banda, K., & Winsemius, H.C. (2020). Evaluation and improvement of remote sensing-based methods for river flow management. *Physics and Chemistry of the Earth, 1474-7065.* doi:10.1016/j.pce.2020.102839

Sammartano, G., & Spanò, A. (2016). DEM Generation based on UAV Photogrammetry Data in Critical Areas. *Proceedings of the 2nd International Conference on Geographical Information Systems Theory, Applications and Management (GISTAM)*, 92-98, ISBN: 978-989-758-188-5. doi:10.5220/0005918400920098

Tiberius, C.C.J.M., Van Leijen, F.J., & Mousivand, A. (2017). *Lecture notes Physical principles of remote sensing: an introduction.* Delft, The Netherlands: TU Delft.

TU Delft. (n.d.). Andreas Krietemeijer. Retrieved April 22nd, 2020, from https://www.tudelft.nl/citg/over-faculteit/afdelingen/watermanagement/staff/staff-water-resources-management/phd-students/andreas-krietemeijer/

TU Delft. (n.d.). Logo. Retrieved April 21st, 2020, from https://www.tudelft.nl/huisstijl/logo/

TWIGA. (n.d.). The Project. Retrieved April 24th, 2020, from https://twiga-h2020.eu/about/index.html

Unavco. (2019). Tutorial: The Geoid and Receiver Measurements. Retrieved May 11th, 2020, from https://www.unavco.org/education/resources/tutorials-and-handouts/tutorials/geoid-gps-receivers.html

Van Til, J. (2018). *TWIGA Flying Sensor Training Flood mapping urban and rural areas.* Retrieved from HiView website: https://www.hiview.nl/publications

Westoby, M.J., Brasington, J., Glasser, N.F., Hambrey, M.J., & Reynolds, J.M. (2012). 'Structure-from-Motion' photogrammetry: A low-cost, effective tool for geoscience applications. *Geomorphology, 179,* 300-314. doi:10.1016/j.geomorph.2012.08.021

Xu, H. (2012). Application of GPS-RTK Technology in the Land Change Survey. *Procedia Engineering, 29,* 3454 – 3459. doi:10.1016/j.proeng.2012.01.511

Zhang, H., Yang, J., Baartman, J.E.M., Li, S., Jin, B., Han, W., Yang, X., Gai, L., Ritsema, C.J., & Geissen, V. (2018). Quality of terrestrial data derived from UAV photogrammetry: A case study of Hetao irrigation district in northern China. *Int J Agric & Biol Eng, 11(3),* 171–177. doi:10.25165/j.ijabe.20181103.3012

Zongjian, L. I. N. (2008). UAV for mapping—low altitude photogrammetric survey. *International Archives of Photogrammetry and Remote Sensing, 37,* 1183-1186.

Picture on cover page shot with the UAV by Jan van Til during the drone flight day.

A. Appendix A: Measure plan Bachelor Thesis

By Ivo van Balen and Ruben Smits

Research topics:

- Retrieval of a digital elevation map using UAV imagery and Ground Control Points collected with a low-cost positioning device;
- Accuracy of a low-cost positioning device, in the horizontal and vertical and for several trajectories.

Location of study area:
Breemwaard, between Zuilichem and Nieuwaal.

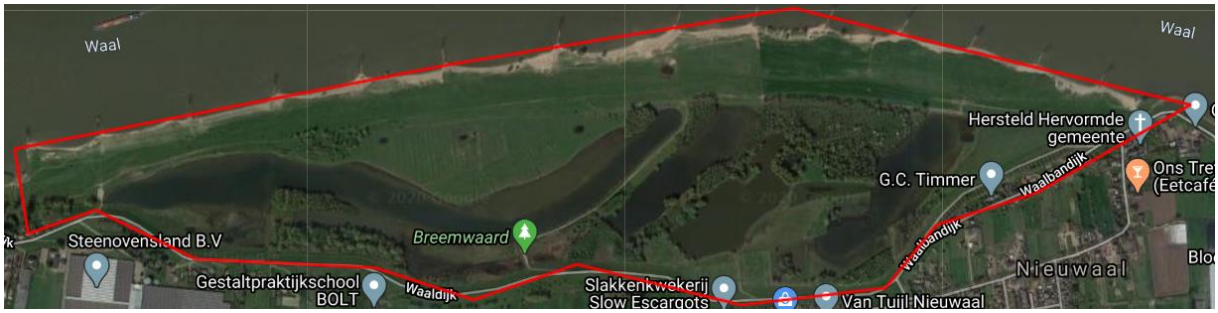

Figure A.1: study area 'Breemwaard' (kmlviewer.nsspot, n.d.)

Introduction

Goal

The goal of the planned measurements is to analyse the differences in accuracy in the measured positions of the ground control points (GCPs) by respectively the low-cost receiver and the professional R8 Trimble. In addition, an elevation model is constructed by using UAV imagery including corrections done by the measurements collected by again the low-cost as well as the professional system.

Insecurities for the accuracy of low-cost positioning device (not in the scope of this report)

In order to research the insecurities and/or inaccuracies of the low-cost positioning device in comparison with the high-end positioning equipment, some specific measurements have to be done.

First of all, the amount of satellites and the presence of obstacles will be properties to be looked at during the doing of the measurements. The goal is to find out how much the availability of satellites affects the accuracy of the positioning measurements. This will be done by noting the degree of 'freedom' around the rover and by noting the amount of satellites that the rover is then connected to. Is the position of the ground control point taken while a lot of obstacles are in the near environment or is there no obstacle to be seen? This level of obstruction has to be noted for every ground control point.
The categories for the obstruction level are:
0 - No obstacles to be found
1 - Only a few obstacles around
2 - Some obstacles blocking the signal
3 - A lot of obstacles that might block the signal

To see if the accuracy of the low-cost positioning device changes when it is used further away from the base station, the distance between the rover and base station will be looked at by placing the base station on a couple (1-2) kilometres in extension on the length of the ground control points. This measurement can also be carried out during another measurement day using the base station of the TU Delft.

Influence factors for the construction of a digital elevation model (DEM)

In addition, a study to influence factors of retrieving a DEM from GCPs is to be done. A few important properties of the GCPs will be tested. Firstly, the number of GCPs is taken into account. This can be determined beforehand and then, the measurements of all the GCPs are done. The influence of it can be checked afterwards. Secondly, the distance between the GCPs can be of impact to the accuracy of the DEM. This will be checked by placing the GCPs with varying distance in the study area. Again, the influence can be checked afterwards. Moreover, in the processing phase, some GCPs can be left out, to study the influence of the spatial distribution of the points on the accuracy, the third aspect to be researched. This aspect does not require an adjusted placement of the GCPs. Lastly, if there is time left, the influence of the gradient of the studied terrain can be checked, as (small) gradients are difficult to capture in a DEM.

Summary

Below, a short overview is given to explain the aims and descriptions of the tests that will be performed. Also, a list of needed equipment is added, which enable the measurements to be carried out.

Necessary materials:

- Trimble R8 receiver including tripod and antenna
- Low-cost receiver including tripod
- Low-cost base station
- Powerbank(s) for electricity
- Markers for the GCPs (wooden piles)
- Large garbage bags as reference points for the drone (1 per marker)
- Measuring tape of at least 10 m
- Pegs (4 per marker)
- Metal plate for antenna base (Peter)
- Metal box to cover antenna
- Plastic box for low-cost base in case of rainfall

Preparations:

- Decision about the set-up of the base station.
- Decision about the boundaries of the area to be studied.
- Decision about the total number of GCPs. (Range: ±20-30.)
    - Preferably a higher number of GCPs than initially needed, in order to enable the study to the influence of total number of GCPs in the processing phase afterwards, and to filter out possible outliers.

Approach:

1. Decided to set up low-cost base station and measure it with the R8 Trimble. Exact position is to be known. According to Andreas Krietemeyer, this method will give a good approximation of the derived location when setting up the low-cost base for 8 hours straight.
2. Determine the exact positions of the GCPs.
    a. The positions depend on the goals of the tests (see below). As described in the introduction, some should be close to obstacles, some should not.
3. Determine the distance between the GCPs. (Range: 100-300m.)
    a. This distance is to be known exactly. Can be measured by hand for an extra check.
4. Start measuring the exact positions of the GCPs using the R8 Trimble and consecutively the low-cost receiver.
5. Send data collected by the Trimble to Hans van der Marel for the processing step.
6. Send data collected by the low-cost device to Andreas.

Test goals:

1. Check the influence of obstacles on the accuracy.
2. Check the influence of number of used satellites on the accuracy.
3. Check the influence of distance between rover and base station on the accuracy.
4. (If possible: check the influence of distance between GCPs on the accuracy - should not affect it, according to Andreas.)

Test goals afterwards:

1. Check the influence of number of GCPs on the accuracy of a DEM.
2. Check the influence of distance between the GCPs on the accuracy of a DEM.
3. Check the influence of the spatial distribution of the GCPs on the accuracy of a DEM.
4. (If possible: check the influence of small gradients in the terrain on the accuracy of a DEM.)

Final tests to perform on site:

All measurements will be performed by both the R8 Trimble and the low-cost receiver.

1. Perform tests with and without the presence of obstacles.
2. Perform tests with a varying number of satellites used.

Possible extra measurements

In addition, a property which is interesting to check is the time-to-first-fix (TTFF) which the rover equipment needs while taking different points. These points will be taken at different locations with different obstruction levels. There will be multiple locations in the same category for which the TTFF will be determined. This will be done on another moment and not during the measurements between 13/5 and 14/5.

Another aspect to be looked at, is the constellations used by the equipment during measurements, this will be noted as well for each of the ground control points.

B. Appendix B: Test scenarios DEM processing

Objective: providing information on generation of an elevation map for local population in Ghana contributing to the TWIGA project.

"How to generate a DEM with an accuracy as high as possible using low-cost positioning devices?"

Part I
Theoretical background on photogrammetry about the retrieval of a DEM from UAV images and measured Ground Control Points (GCPs).

Part II
Possible influence factors for accuracy:

- The total number of measured GCPs used in the processing phase;
- The distance between the measured GCPs used in the processing phase;
- The spatial distribution of the measured GCPs used in the processing phase.

Questions of relevance:

- How should the influence factors be filled in and divided in order to achieve the highest accuracy for a DEM?
- Which influence factor affects the accuracy the most?

Specific case in study area the Breemwaard:
19 GCPs, distributed in a raster of 2-3-3-4-4-3 markers in a row. Intermediate distances differ between 50 and 150 metres.

Figure B.1: study area including the positions of the measured GCPs (Google Maps, 2020).

Processing scenarios during construction of a DEM, combining the influence factors:

- Scenario 1: use all GCPs;
- Scenario 2: only use four GCPs on the edges of the area (3, 6, 16, 19);
- Scenario 3: use none of the GCPs.

With these scenarios having been tested, hopefully conclusions can be derived about the effects of the three influence factors.

C. Appendix C: Retrieved DEMs

Below, the retrieved DEM of scenario 1 (only UBlox) and scenario 2 are shown. As mentioned in paragraph 4.1, the visible differences between the DEMs of scenario 1 and 2 are little. Only the white parts, representing large trees, differ slightly due to the fact that some vegetation was manually removed in the generation process. This led to a different representation of the vegetation.

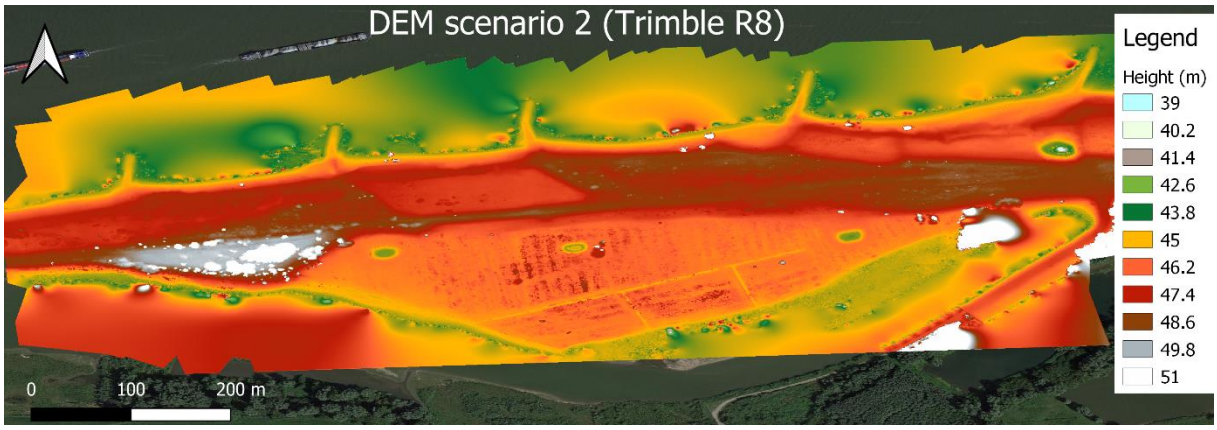

Figure C.1: DEM in scenario 2 from the Trimble R8 data, generated with the use of 4 GCPs

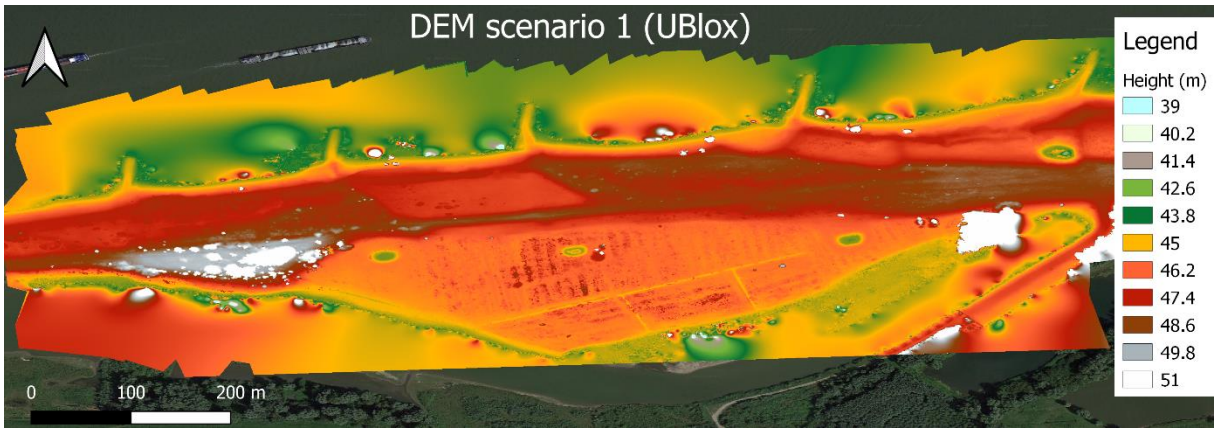

Figure C.2: DEM in scenario 1 from the UBlox data, generated with the use of 19 GCPs.

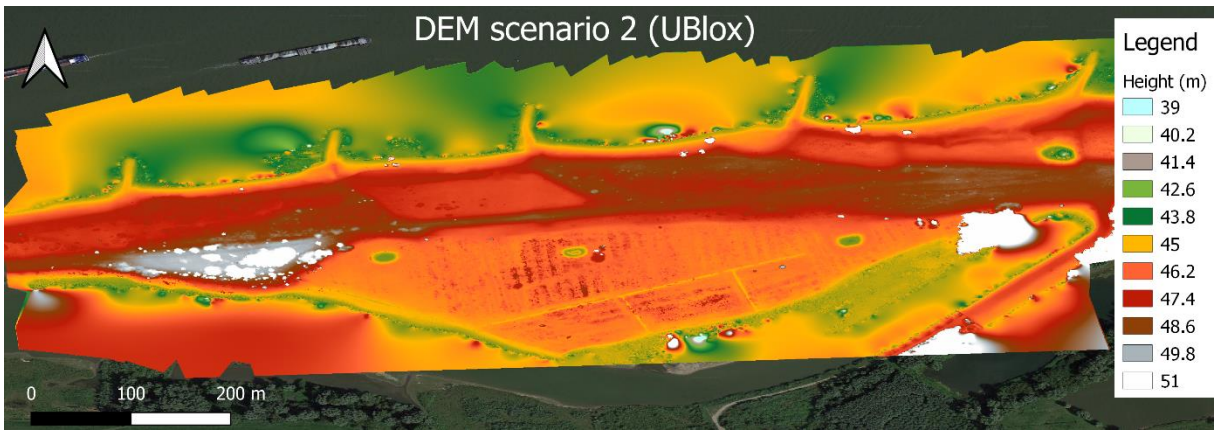

Figure C.3: DEM in scenario 2 from the UBlox data, generated with the use of 4 GCPs

D. Appendix D: Results

In the following tables, all the measured elevation values on the studied points per different scenario are presented. The values in Table D.1 represent the orthometric height in WGS84 and are all given in metres. Table D.2 is one of the tables used for the analysis of deviations between the different generated DEMs. The minimum and maximum errors of the studied points were calculated as well as the mean absolute error (MAE) and the root mean squared error (RMSE). The colour scheme also shows where the highest errors occur.

	Trimble DEM s1	Ublox DEM s1	Trimble DEM s2	Ublox DEM s2	DEM s3
1	47.525818	47.527115	47.524426	47.521328	46.521027
2	47.653862	47.626057	47.647873	47.613773	46.66547
3	47.826023	47.784447	47.82875	47.805264	46.81481
4	47.797493	47.7754	47.829422	47.808975	46.846024
5	47.49578	47.50163	47.601284	47.56113	46.66279
6	48.160194	48.16828	48.2332	48.207348	47.295834
7	47.28785	47.29853	47.36473	47.356182	46.493187
8	46.812275	46.819416	46.855137	46.8296	46.016678
9	47.622253	47.617714	47.62061	47.59133	46.68192
10	48.415836	48.40392	48.429924	48.393177	47.57484
11	48.53527	48.53112	48.525776	48.51368	47.695084
12	48.413967	48.40791	48.422768	48.421593	47.689793
13	46.471222	46.484085	46.46353	46.500294	45.712936
14	46.53246	46.53904	46.481766	46.522167	45.703556
15	46.447342	46.44508	46.323677	46.37486	45.533916
16	48.72232	48.72838	48.577427	48.637367	47.921085
17	48.4314	48.429234	48.40145	48.43522	47.736546
18	48.2566	48.253616	48.247074	48.239967	47.522617
19	48.252975	48.237682	48.230644	48.203575	47.465504
20	48.836414	48.840424	48.849197	48.8097	48.063618
21	48.738876	48.72516	48.729824	48.678448	47.89963
22	48.44663	48.439552	48.432743	48.408184	47.629944
23	49.634186	49.626446	49.706642	49.67602	48.851105
24	49.759262	49.752464	49.781666	49.75425	48.825516
25	48.46226	48.471806	48.455902	48.433247	47.494854
26	45.588684	45.57898	45.65824	45.617332	44.82805
27	45.612606	45.551838	45.737125	45.69559	44.828335
28	45.475677	45.417774	45.530483	45.492188	44.67911
29	45.777283	45.751385	45.7935	45.761143	45.02531
30	45.937157	45.90258	45.93303	45.91046	45.151463
31	46.03984	46.014503	46.018696	45.97657	45.238686
32	46.08252	46.074436	46.088543	46.03775	45.317093
33	46.065865	46.060406	46.074406	46.02832	45.35441
34	46.27721	46.252174	46.279827	46.249466	45.54521
35	46.569324	46.578667	46.560795	46.534546	45.868107
36	46.507458	46.506268	46.495758	46.47337	45.792458
37	47.04973	47.06248	47.055817	47.050785	46.36703

38	47.624477	47.638405	47.579865	47.59747	46.895416
39	48.126293	48.149727	47.968807	48.00961	47.320545
40	45.430195	45.445156	45.415634	45.441647	44.86304
41	45.89537	45.88832	45.883514	45.887012	45.195255
42	45.880547	45.89108	45.885906	45.85946	45.256756
43	45.881435	45.85828	45.8804	45.834515	45.221924
44	45.669754	45.641712	45.721367	45.666862	45.016674
45	45.348698	45.28889	45.385246	45.34836	44.580776
46	45.404976	45.338036	45.43029	45.392048	44.617573
47	45.3347	45.295574	45.341614	45.308765	44.658302
48	45.504017	45.484425	45.541668	45.49961	44.89911
49	45.61671	45.595802	45.66322	45.623634	45.035812
50	45.40508	45.37635	45.452892	45.397465	44.835564
51	45.37182	45.331535	45.348312	45.315113	44.776695
52	45.40222	45.383015	45.380573	45.330578	44.80845
53	45.347614	45.3452	45.314964	45.29055	44.735973
54	45.408924	45.396362	45.389366	45.387234	44.815334
	46.89212504	**46.88025681**	**46.89583889**	**46.87618763**	**46.12679157**

45.3347	**45.28889**	**45.314964**	**45.29055**	**44.580776**	min
49.759262	**49.752464**	**49.781666**	**49.75425**	**48.851105**	max

Table D.1: measured elevation values from the DEMs in QGIS, per studied point.

Trimble s1 - Ublox s1	**Trimble s1 - Ublox s1**	**Trimble s1 - Ublox s1**
error	absolute error	squared error
-0.001297	0.001297	1.68221E-06
0.027805	0.027805	0.000773118
0.041576	0.041576	0.001728564
0.022093	0.022093	0.000488101
-0.00585	0.00585	3.42225E-05
-0.008086	0.008086	6.53834E-05
-0.01068	0.01068	0.000114062
-0.007141	0.007141	5.09939E-05
0.004539	0.004539	2.06025E-05
0.011916	0.011916	0.000141991
0.00415	0.00415	1.72225E-05
0.006057	0.006057	3.66872E-05
-0.012863	0.012863	0.000165457
-0.00658	0.00658	4.32964E-05
0.002262	0.002262	5.11664E-06
-0.00606	0.00606	3.67236E-05
0.002166	0.002166	4.69156E-06
0.002984	0.002984	8.90426E-06
0.015293	0.015293	0.000233876
-0.00401	0.00401	1.60801E-05
0.013716	0.013716	0.000188129
0.007078	0.007078	5.00981E-05

0.00774	0.00774	5.99076E-05
0.006798	0.006798	4.62128E-05
-0.009546	0.009546	9.11261E-05
0.009704	0.009704	9.41676E-05
0.060768	0.060768	0.00369275
0.057903	0.057903	0.003352757
0.025898	0.025898	0.000670706
0.034577	0.034577	0.001195569
0.025337	0.025337	0.000641964
0.008084	0.008084	6.53511E-05
0.005459	0.005459	2.98007E-05
0.025036	0.025036	0.000626801
-0.009343	0.009343	8.72916E-05
0.00119	0.00119	1.4161E-06
-0.01275	0.01275	0.000162563
-0.013928	0.013928	0.000193989
-0.023434	0.023434	0.000549152
-0.014961	0.014961	0.000223832
0.00705	0.00705	4.97025E-05
-0.010533	0.010533	0.000110944
0.023155	0.023155	0.000536154
0.028042	0.028042	0.000786354
0.059808	0.059808	0.003576997
0.06694	0.06694	0.004480964
0.039126	0.039126	0.001530844
0.019592	0.019592	0.000383846
0.020908	0.020908	0.000437144
0.02873	0.02873	0.000825413
0.040285	0.040285	0.001622881
0.019205	0.019205	0.000368832
0.002414	0.002414	5.8274E-06
0.012562	0.012562	0.000157804
0.011868222	**0.017685333**	**0.023914998**
	MAE	**RMSE**

-0.023434	min
0.06694	max

Table D.2: one of the tables with error analysis between the different DEMs per studied point.

E. Appendix E: DEM comparison

In addition to the analysis of the UBlox DEMs relative to the reference DEM, other comparisons between all of the other derived DEMs were made. The results are shown in Table E.1. The results of Table 4.1 are visible in this table as well. A few remarkable results were found in this analysis.

	Max negative error	**Max positive error**	**MAE**	**RMSE**
Trimble scen1 – Trimble scen2	-0.124519	0.157486	0.033676037	0.050352614
Ublox scen1 – Ublox scen2	-0.143752	0.140117	0.033630111	0.044566219
Trimble scen1 – Ublox scen1	-0.023434	0.06694	0.017685333	0.023914998
Trimble scen2 – Ublox scen2	-0.05994	0.055427	0.031131889	0.034323521
Trimble scen1 – Ublox scen2	-0.082984	0.116683	0.032217741	0.040827899
Trimble scen2 – Ublox scen1	-0.18092	0.185287	0.044321926	0.062702543
Trimble scen1 – scen3	n/a (min positive: 0.567155)	1.011213	0.765333463	0.773785578
Trimble scen2 – scen3	n/a (min positive: 0.552594)	1.01394	0.769047315	0.778786114
Ublox scen1 – scen3	n/a (min positive: 0.540786)	1.006088	0.753465241	0.762421954
Ublox scen2 – scen3	n/a (min positive: 0.522128)	1.000301	0.749396056	0.759148672

Table E.1: comparisons between all the different DEMs.

- First, it is visible that the deviations between the Trimble R8 and UBlox DEMs are very small not only in scenario 1, but also in scenario 2. In scenario 2, the MAE and RMSE do increase with factors 1.76 and 1.44, but the number of GCPs decreased with a significantly higher factor of 4.75. This means that for a lot of purposes, the UBlox receiver is a good alternative to the Trimble device.
- It can also be stated that the more GCPs are used in the generation phase, the more accurate the model will be. The UBlox DEM in scenario 1 (19 GCPs) performs considerably better than the Trimble DEM in scenario 2 (4 GCPs).
- Relative to the Trimble scenario 1 DEM, the UBlox scenario 2 DEM is highly comparable with the Trimble scenario 2 DEM, or even better.
- Finally, it can be seen that the differences between the UBlox scenario 1 and 2 are comparable with the differences between the Trimble scenario 1 and 2. This can mean that the effect of a lower number of GCPs influences the UBlox and Trimble devices in a similar way.

F. Appendix F: Accuracy GCPs versus interpolated points

Due to the fact that the DEMs are corrected by the positional information of the GCPs, it is assumed that the accuracy on that location in the elevation map is higher. Therefore, in this research only the results of interpolated points which are constructed by the photogrammetric software were analysed. In Table F.1 and F.2, however, the accuracy of the interpolated points as well as the accuracy of the positions of the GCPs in each scenario are shown, relatively to the reference DEM. These results show that, overall, the errors of the interpolated points are actually similar with the errors of the 19 GCPs. Only the maximum positive and negative errors seem to be considerably lower for the positions of the GCPs. It is also clearly visible that the MAE and RMSE of the GCPs increase in scenario 2 with respect to scenario 1 and even become larger than the MAE and RMSE of the interpolated points. This can be caused by the fact that scenario 2 uses only four of the GCPs to be corrected with, resulting in more points to be interpolated by the photogrammetric software.

	Number of GCPs		
	19	**4**	**0**
GCPs per hectare	0.70	0.15	0
Max positive elevation error	0.023434	0.082984	- (min negative: -0.567155)
Max negative elevation error	-0.06694	-0.116683	-1.011213
Mean absolute elevation error	0.017685333	0.032217741	0.765333463
Root mean squared error	0.023914998	0.040827899	0.773785578

Table F.1: error analysis of the 54 random chosen points spread over the study area.

	Number of GCPs		
	19	**4**	**0**
GCPs per hectare	0.70	0.15	0
Max positive elevation error	0.014187	0.043624	-
Max negative elevation error	-0.054026	-0.080625	-
Mean absolute elevation error	0.015819263	0.037387789	-
Root mean squared error	0.022287436	0.04330033	-

Table F.2: error analysis of the 19 GCPs in the study area.